

Time of Emergence of Precipitation Change in Sudan and South Sudan

By

Almokashfi Algiliy Omer (almokashfi.algiliy@aims.ac.rw)

الكافي الحيلي عمر حامد

African Institute for Mathematical Sciences (AIMS), Rwanda

Supervised by: Dr. Mouhamadou Bamba SYLLA

African Institute for Mathematical Sciences (AIMS), Rwanda

June 2022

*AN ESSAY PRESENTED TO AIMS RWANDA IN PARTIAL FULFILMENT OF THE REQUIREMENTS FOR THE AWARD OF
MASTER OF SCIENCE IN MATHEMATICAL SCIENCES*



DECLARATION

This work was carried out at AIMS Rwanda in partial fulfilment of the requirements for a Master of Science Degree.

I hereby declare that except where due acknowledgement is made, this work has never been presented wholly or in part for the award of a degree at AIMS Rwanda or any other University.

Student: Almokashfi Algiliy Omer

A handwritten signature in blue ink, appearing to read "Almokashfi Algiliy Omer".

ACKNOWLEDGEMENTS

I'd like to thank Dr. Mouhamadou Bamba SYLLA, the AIMS-Canada Research Chair in Climate Change Science for agreeing to supervise this dissertation and for his critical thinking and orientation that have contributed significantly to the project's success. My thanks also go to the AIMS Rwanda staff in general for all of their assistance throughout the program. I would especially like to thank my tutor, Mr Joel Pascal, for all that he has contributed to this work. I also want to thank my dear friends and colleagues from the AIMS Rwanda 2021 cohort for their contributions, which included numerous exchanges and criticisms. And I'd like to hire specialists Mazin Abdoalatif and Yves Heri. This work is dedicated to my family, who have always supported me and prayed for me. I'd like to thank my mother, Souad Mohamed, and father, Algiliy Omer, in particular. Dear Dr. Ayman Hamid, I hope to always honor you with my journey and pass on what I've learned from you. Finally, I give thanks to the most high for guiding, supporting, and strengthening me over the years.

Abstract

The time of emergence (ToE) of climate change is the time when climate change causes variables to differ from what they have been in the past variability. ToE evaluation is particularly important in Sudan and South Sudan, which are extremely vulnerable to climate change and in desperate need of reliable climate forecasts. In this study, we assessed the ToE of the change in precipitation in Sudan and South Sudan by using the signal-to-noise ratio method based on three precipitation indices: the frequency of wet days, the annual mean precipitation, and the number of heavy precipitation days. The analyses were based on simulated data from the MPI-ESM1-2-HR climate model. Our results showed a late emergence in the frequency of wet days (after 2080), whereas the ToE of the annual mean precipitation and number of heavy precipitation days will be within the next two decades of the twenty-first century. ToEs for all precipitation indices are expected before 2040 in many areas of central Sudan. However, ToEs of the change in the annual mean precipitation and frequency of wet days fall within the early twenty-first century, before 2020, in South Sudan. ToE assessment for the number of heavy precipitation days showed that change had already happened as a result of natural variation in the 20th century. This shows that Sudan will be more vulnerable to climate change than South Sudan in the 21st century.

Contents

Declaration	i
Acknowledgements	ii
Abstract	iii
1 Introduction	1
1.1 Background of the study	1
1.2 Problem statement	2
1.3 Aim of the study	3
1.4 Overview	3
2 Literature Review	4
3 Data and Methods	6
3.1 Area of study	6
3.2 Climatology of the area	7
3.3 Data processing	8
3.4 Physical description of climate models	10
3.5 Model considered	14
3.6 Climate projection	15
3.7 Estimating the Time of Emergence (ToE)	15
4 Result and Discussion	20
4.1 Projected change in the frequency of wet days	20
4.2 The ToE of change in the frequency of wet days	21
4.3 Projected change in the annual mean precipitation	22
4.4 The ToE of the change in the annual mean precipitation	24
4.5 Projected change in the number of heavy precipitation days	25
4.6 The ToE of the change in the number of heavy precipitation days	26

5 Conclusion 28

References 32

List of Figures

3.1	Topography of Sudan and South Sudan (Zumrawi and Hamza, 2014)	6
3.2	Time series of global mean precipitation changes in percentage (Sung et al., 2021)	8
3.3	Flow chart indicating data sources, steps, and outputs for ToE.	19
4.1	Projected change in the frequency of wet days in Sudan and South Sudan . . .	21
4.2	The ToE of change in the frequency of wet days in Sudan and South Sudan .	22
4.3	Projected changes of annual mean precipitation in Sudan and South Sudan . .	23
4.4	The ToE of the change in the annual mean precipitation	24
4.5	Projected change in the number of heavy precipitation days in Sudan and South Sudan	26
4.6	Time of Emergence of the heavy days precipitation	27

List of Tables

3.1 Data classification	9
3.2 Precipitation indices	9

List of Abbreviations

ToE	Time of Emergence
SDG	Sustainable Development Goal
IPCC	The Intergovernmental Panel on Climate Change
WCRP	The World Climate Research Program
CIMP	The Coupled Model Intercomparison Project
CIMP6	The Coupled Model Intercomparison Project 6th phase
SSP	Shared Socioeconomic Pathways
RCP	Representative Concentration Pathway
KS	Kolmogorov-Smirnov
IFRC	International Federation of Red Cross and Crescent Societies
CDO	Climate Data Operators
NetCDF	Network Common Data Form
CWD	Consecutive wet days
R10mm	Number of heavy precipitation days
Yearmean	Mean precipitation
ETCCDI	Expert Team on Climate Change Detection and Indices
ESGF	Earth System Grid Federation

1. Introduction

1.1 Background of the study

Climate change is a concept that is gradually gaining prominence over the last couple of years mainly due to the perceived possible consequences on the planet. It is of relative importance being the 13th Sustainable Development Goal (SDG) in the 2030 Agenda for Sustainable Development, and it is seen that the other SDGs are affected by climate change ([Zhenmin and Espinosa, 2019](#)). It is indisputable that climatic conditions in recent years tend to grow into undesirable situations due to natural forces as well as human activities on land that result in an overall increase in the global temperature. These activities include the burning of fossil fuels, continuous emission of greenhouse gases, and so on ([Singh and Singh, 2012](#)). The consequence of adverse climatic conditions is climate disasters such as floods, drought, heatwaves, etc. These are continually affecting human needs thereby exposing humans to challenges like poverty, food insecurity and water scarcity, among others.

Sudan and South Sudan, like any other part of the world, have experienced numerous environmental changes over time; some of these changes are currently taking place, while others will likely come in the future as a result of ongoing activities ([Rhodes, 2012](#)). Rainfall, for example, is volatile and varies greatly from the north of Sudan to the south. As a result, the rain-fed agricultural system is more susceptible because of the capriciousness of rainfall and its peak during the short growing season. Drought conditions are aggravated in many regions of the country by decreasing annual rainfall, as well as increased rainfall variability([Elfaig et al., 2013](#)).

To anticipate and alleviate possible climatic disasters, it is essential to determine the Time of Emergence (ToE) which is the time when climate variables begin to change from what they had been in the past because of natural variation at a given location ([Gaetani et al., 2020](#)). The significance of assessing the ToE in Sudan and South Sudan cannot be overemphasized due to the fact that an accurate estimate is highly relevant in prioritizing both alleviation and acclimatization activities in areas expecting rigorous climate change. Moreover, this is vital since populations are heavily dependent on rain-fed agriculture and thus, they are usually more exposed to climate change ([Nimir and Elgizouli, 2013](#)).

Addressing climate change requires climate and earth system models, which are highly complex computer programs that allow us to study the Earth's system and predict future climate ([Goosse et al., 2010](#)). These models aid in the study and prediction of climate, and as a result, they are improved on a regular basis by the groups in charge of modelling climate change over time. The updated versions are based on the schedule of The Intergovernmental Panel on Climate Change (IPCC) Assessment Reports, providing users with models that adhere to the same standards and structure ([Change, 2014](#)).

The World Climate Research Program (WCRP) allows scientists to compare and share their models through an inter-comparison initiative. The Coupled Model Intercomparison Project is the name given to this initiative (CMIP). The CMIP establishes research guidelines and processes, by following these and employing the same climate change scenarios. The outcomes are used

for understanding climates such as precipitation and temperature which are very important to agriculture and human living conditions. CIMP has different three phases, CMIP3, CIMP5 and CIMP6. The researchers attempted to develop CIMP5 while also resolving many different issues in CIMP5 on their Representative Concentration Pathway (RCP) scenarios, as a result, they create new scenarios in CIMP6 that takes the name SSP which stands for Shared Socioeconomic Pathways and based on different economic and social assumptions made by the energy modelling community. Emissions scenarios (SSPs) are expected to have a significant impact on projections of future climate change, including precipitation (Eyring et al., 2016).

A climate emergency is defined as a scenario in which immediate action is needed to slow or stop climate change and prevent potentially permanent environmental damage (Oxford University , 2019). It is the responsibility of the government and scientists to declare that humanity is facing a climate emergency. The next stage is to prioritize climate change mitigation, which is where ToE assessments play a crucial role. ToE assessments aid in climate alleviate by providing useful information on the point at which the climate begins to change, which makes climate alleviate processes simple to manage it. Furthermore, when used in climate models, ToE assessment considers differences in model design and performance, as well as the emission scenario chosen, which aids in improving model performance (Gaetani et al., 2020).

1.2 Problem statement

Many countries, including Sudan and South Sudan, are exposed to the effects of climate change, both countries are heavily reliant on agriculture and the pastoral system, which are considered the primary means of income in rural areas according to a study conducted by Zakieldeen (2009). Rainfall variability has increased in recent decades, putting strain on the region's rainfed agriculture and pastoralist systems, which are the primary sources of income in rural regions (Elfaig et al., 2013). Variability in rainfall also leads to unreliable food yields and diminishing productive land and water resources, where the consequences of severe weather events in 2007 were tragic. Early, prolonged, and heavy rains caused devastating flooding, affecting over 500,000 people. Over 200 people have died as a result of diseases spread by contaminated water and poor hygiene standards (IFRC, 2010). Based on these facts, knowing when and where the climate would change in Sudan and South Sudan in respect of their time of emergence is critical, to alleviating the consequences of precipitation variability and general climatic change.

1.3 Aim of the study

The main objective of this study is to determine the time of emergence (ToE) in precipitation change in Sudan and South Sudan. More specifically, this study aims to:

1. Develop precipitation indices.
2. Assess the projected change in each of the precipitation indices.
3. Develop a method for determining the time of emergence.
4. Determine the time of emergence based on each precipitation index.

1.4 Overview

The following is how the essay is structured: The second chapter is devoted to a review of relevant literature. Chapter 3 gives an overview of climate models and explains the methodology that will be used throughout the project. The results and discussion are presented in Chapter 4. Finally, Chapter 5 summarizes the study's findings and suggests future research directions.

2. Literature Review

The concept of emergence has different definitions in different fields, it's defined based on the field of study of interest which refers to the existence or formation of collective behaviours. In this study, our interest in the field of climate science, which uses the Time of Emergence (ToE) variably to find the emergence in many aspects of climate and its components. Hence, various studies on the Time of Emergence (ToE) have recently been conducted, with different study areas including Africa, Asia, and Europe.

Hence, [Giorgi and Bi \(2009\)](#) defined the ToE in twenty-first century projections, as the time when the magnitude of the ensemble mean precipitation change signal exceeds the uncertainty because of inter-model spread and internal model multi-decadal variability. The study's main goal was to evaluate the ToEs of 14 green-house gases that caused precipitation changes in their 14 locations around the world. The assessment for the ToE of green-house gases was based on the multi model ensemble CMIP3, by using the signal-to-noise method, which is a very common method for assessing the ToEs. As a result, they found that six of the greenhouse gases have a ToE in the early twenty-first century, three in the middle, and five in the late.

Also, there is a different definition for ToEs across the climate components; the previous work defined the ToE based on uncertainty due to differences in model outputs, but [Lyu et al. \(2014\)](#) defined the ToE basis of greenhouse growth and decrease as the point at which the signal of climate change caused by increasing greenhouse gas emissions outpaces the signal caused by decreasing greenhouse gas emissions. The primary goal of this research was to estimate the ToEs of sea-level rise using a signal-to-noise threshold. According to the study's findings, as the sea levels rise, 50% of the ocean area will be revealed from the early to mid-forties. More than half of the ocean will have surfaced by 2020. What distinguishes this work from previous research is that it focuses on the ocean rather than the atmosphere.

Furthermore, [Sui et al. \(2014\)](#) used two different atmospheric variables to estimate the ToE: precipitation and surface air temperature over China. By using signal to noise ratio method based on 30 climate models. The study's findings were as, in the eastern Qinghai-Tibetan Plateau, the annual and seasonal temperature ToE between 2006 and 2012 for the signal to noise ratio greater than one, and between 2020 and 2030 for a ratio greater than two regards surface air temperature. Thus, for precipitation and regard to the annual mean, the early ToE occurs in the northeastern Qinghai-Tibetan Plateau. And it occurs primarily in the winters of northern Northeast China and southern Northwest China, as well as in the winters and springs of the northeastern Qinghai-Tibetan Plateau. Southern China's median ToE will not be reached until 2090.

Despite the fact that much previous work has concentrated on assessing ToE, [Hawkins and Sutton \(2012\)](#) presents a methodology (signal to noise ratio) for assessing ToE for specific climate models and measuring the uncertainty of their findings. They used this methodology to generate maps of surface air temperature change for ToE. The noise in the method is defined as the standard deviation between years for seasonal or annual means. In contrast, the signal is first regressed using a single ensemble member's variable surface air temperature for each model in each grid

box. Thus, the definition of ToE becomes based on this methodology which is the time when the signal to noise ratio exceeds a threshold they set. The findings of the study revealed that median ToE occurs several decades earlier in boreal summer in low latitudes than in mid-latitudes. They also show that the median ToE occurs earlier in the winter than in the summer in the Arctic. ToE is uncertain for at least the next 30 years, and in some cases reach up to 60 years.

In addition, [Chadwick et al. \(2019\)](#) presented a methodology for calculating the ToEs of changes in precipitation and temperature at local scales over Chile. To evaluate ToE, the methodology considers both the climate and the projections of unbiased GCMs. The method works by using statistical power to determine when the climate is significantly different from the historical one. According to the study, ToE has already occurred for temperature in three Chilean basins: Limar, Maipo, and Maule. However, an earlier ToE for the Maule basin is clearly identified in terms of precipitation.

Most previous works used individual methods (signal-to-noise ratio) to assess ToE in contrast to [Im et al. \(2021\)](#) used three different methods to estimate the ToE of temperature and wet-bulb temperature; two different signal-to-noise structure and the Kolmogorov– Smirnov test (KS). Utilizing RCP2.6 and RCP8.5 projections of the fine-scale, long-term regional climate model. The study's findings are as follows: under RCP8.5, the land fraction exposed to ToE is expected to exceed 90 % by the middle of the next decades in 2050s, whereas under RCP2.6, the increase rate of land exposure to ToE tends to stagnate over time, so that more than 40 % of land will not be exposed to ToE by the end of the 21st century.

Furthermore, [Gaetani et al. \(2020\)](#) assessed the ToE of the change in precipitation matrix over West Africa by using three methods, as in the previous work: the Kolmogorov-Smirnov (KS) test, smoothing, and linear trend analysis. The ToE is estimated using five precipitation indices: the number of wet and very wet days, the start and length of the rainy season and the accumulated precipitation. The study's finding of ToEs analysis in West Sahel revealed an early occurrence of wet days prior to 2036. The East Sahel ToEs Assessment found that very wet days are likely to occur before 2054. The findings do not provide a clear indication of a potential climate shift in terms of the onset and duration of the rainy season.

3. Data and Methods

3.1 Area of study

Sudan and South Sudan cover a large and diverse geographical area with a variety of climatic conditions. Sudan is located in Northeast Africa, with a natural climate ranging from sand and gravel-clad desert in the north to arid and semi-arid areas in the centre and tropical rainforests in the south. Sudan borders seven countries: Libya, Egypt, Chad, the Central African Republic, South Sudan, Ethiopia, and Eritrea. On the other hand, South Sudan is a landlocked Central African country near the equator with a tropical climate and tropical rainforests. South Sudan is surrounded by six countries on all sides. Sudan, Ethiopia, Kenya, Uganda, the Democratic Republic of the Congo, and the Central African Republic ([Mohamed and El-Mahdy, 2021](#)).

The latitude and longitude of Sudan are $12.8628^{\circ}N$ and $30.2176^{\circ}E$, respectively. Sudan has a current population of 45,844,370 and an area of $1,886,068km^2$, making it Africa's third-largest country by area. South Sudan's latitude and longitude are $6.8770^{\circ}N$ and $31.3070^{\circ}E$, with a current population of 11,588,161 and an area of $644,329, km^2$ ([World Population Review, 2022](#)).

Figure 3.1 shows a map of Sudan and South Sudan that depicts the terrain, as well as the north Sudanese desert region and the Nile River and its tributaries.



Figure 3.1: Topography of Sudan and South Sudan ([Zumrawi and Hamza, 2014](#))

3.2 Climatology of the area

Rainfall

Rainfall is regarded as the most significant atmospheric variable, particularly in Africa. Rainfall is required to support the Sudanese and South Sudanese peoples' livelihoods, as agriculture is heavily reliant on rainfall in both countries. Throughout the year, the north of Sudan is primarily arid, with annual rainfall averaging less than 50 mm (nearly nothing). However, areas near the Red Sea coast receive some rainfall during the boreal winter, whereas the country's centre is semi-arid, receiving between 200 and 700 mm of rain per year. The rainy season in the region lasts from March to October, with the greatest concentration between June and September. South Sudan shares some characteristics with the equatorial east African bimodal rainfall regime, with annual rainfall averaging 700 to 1,300 mm, with the majority falling during the summer months. The rainy season lasts from June to September, and the dry season lasts from October to April. Rainfall is increasing across the region, from South Sudan to North Sudan (Rhodes, 2012).

Temperature

Sudan and South Sudan are often regarded as among Africa's hottest countries throughout the year. Regarding Sudan, which is considered a very hot country throughout the year, the maximum temperature record in this country exceeds 43.3°C during the summer in the north and the annual average temperature is ranges between 26°C and 32°C while the minimum temperature record is below 13.75°C . Summer is the hottest season, and lasts from July and to September (Climate Change Knowledge Portal, 2022).

The climate of South Sudan is tropical and hot. The maximum temperature record exceeds 35°C during the dry season and the annual average temperature is ranges between $26 - 32^{\circ}\text{C}$, while the minimum temperature record was below 11.2°C . Summer is the hottest season, and lasts from July and to September. The average temperature have risen by $1 - 1.5^{\circ}\text{C}$ since the 1970s (Colin Quinn and Habib, 2019).

Topography of the area

Sudan is a large and diverse plain, and the northern part of Sudan is divided into two distinct parts: the Sahara (the Nubian Desert lies to the east of the Nile, while the Libyan Desert lies to the west) and the Nile River (the northern part) which is the longest river in the world. Sudan contains many mountains scattered in different places such as the Marra Mountains in western Sudan, and widely scattered mountain ranges such as the Nuba Hills, an area located in South Kordofan in Sudan. The sandy wastelands to the west and the Red Sea Hills to the east. (Wikipedia contributors, 2022).

The majority of South Sudan consists of plateaus, plains, mountains (e.g Didinga Hills, Dongotona Mountains and Imatong.) and highland areas that can be found all over the country, especially near the country's borders while the center of the country is vast and plain .The Imatong Mountains are located in South Sudan's southeast. The range has an equatorial climate and has dense forests supporting diverse wildlife (Fernando and Garvey, 2013).

3.3 Data processing

3.3.1 Data description. The Coupled Model Intercomparison Project 6th phase (CMIP6) database was used for the study. The output of the MPI-ESM1-2-HR model, which is a higher resolution version of the Max Planck Institute Earth System Model, The datasets are split into two categories: historical and projection. The model data has a high-resolution grid that covers all of Africa between 1850 and 2014 for historical experiments. For Experiments on climate projection, we used the Shared Socioeconomic Pathway (SSP) which provides data for the period 2006–2300, but in this study, the period of interest in order to calculate the precipitation indices was 2015–2100. The datasets are available on the Earth System Grid Federation (ESGF) data server, where they can be found by searching the model name and reference ¹.

Future scenarios description Socioeconomic pathways that are shared by the SSP describe how the social and economic landscape may change in the future. The different standards that are likely to occur when there is no concentrated international effort to combat climate change are defined by different levels of green-house gases and radiative forces. SSPs are intended to reflect a wide range of mitigation and adaptation challenges, from low to very high. The SSPs are built around five scenarios that describe the major socioeconomic trends that may shape society in the future. These are meant to broaden the logical future's scope and include global equity and long-term growth. SSP1 is an intermediate world in which trends follow historical patterns. A world of rising nationalism is divided by SSP2. SSP3 represents a world with growing inequalities. SSP4 represents a world with unrestricted economic production and energy consumption. The SSP5 scenario is the pinnacle of the literature on fossil fuel consumption, food demand, energy consumption, and greenhouse gas emissions (Riahi et al., 2017). Hence, in this study we choose SSP2-4.5 and SSP5-8.5 as future scenarios. Figure 3.2 depicts a time series of percentage changes in global mean precipitation.

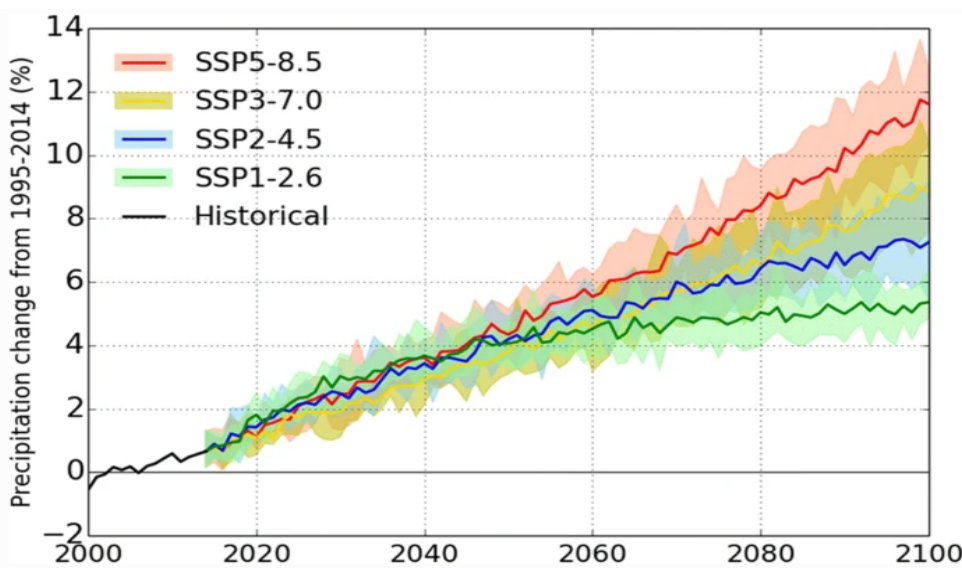


Figure 3.2: Time series of global mean precipitation changes in percentage (Sung et al., 2021)

¹Earth System Grid Federation (ESGF) <https://esg-dn1.nsc.liu.se/search/cmip6-liu/>

3.3.2 Data extraction. The data is a high-resolution grid covering the entire African continent, but we are only interested in Sudan and South Sudan. Datasets are saved in network Common Data Form (NetCDF) format and can be explored using the Climate Data Operators (CDO) software. We extracted the data for study domain based on the area's latitude and longitude.

The CMIP6 historical data set ranges from 1950 to 2014. We used the Socioeconomic Shared Pathway (SSP) data set for climate projection experiments, which includes data from 2015 to 2100. The study period of interest for assessing the ToEs in this study ranged from 1950 to 2100.

Tabel 3.1 depicts the data classification used in this research study.

Table 3.1: Data classification

Experiments	Variable	Nominal Resolution	Temporal Resolution
Historical (1950-2014)	Precipitation	100 km	daily
SSP2-4.5 (2015-2100)	Precipitation	100 km	daily
SSP5-8.5 (2015-2100)	Precipitation	100 km	daily

3.3.3 Selected precipitation indices. Tabel 3.2 below shows the precipitation indices used in this study. We chose the indices because they provide a comprehensive overview of precipitation statistics to assess changes in the duration (the length of time that something lasts), intensity and incidence of precipitation. These indices were calculated using a combination of CDO commands and Climpact data². The precipitation indices were defined by the Expert Team on Climate Change Detection and Indices (ETCCDI) (Quenum et al., 2021).

Table 3.2: Precipitation indices

Index	Description Name	Definition	Units
CWD	Consecutive wet days	Maximum number of consecutive wet days	day
R10mm	Number of heavy precipitation days	Annual count of days when RR > 10 mm	day
Yearmean	Mean precipitation	Annual average precipitation per year	mm/year

² <https://climpact-sci.org/indices/>

3.4 Physical description of climate models

Climate models can be defined as numerical representations of fundamental equations used to predict long-term trends and project climate changes. They are built by combining fundamental laws of physics, biology, and chemistry into a mathematical model that describes the behavior of the climate system and the interactions between its components, that is the atmosphere, ocean, cryosphere, biosphere, and the chemosphere. These models can be computed mathematically, specifically in the theory of partial differential equations, and can represent the time rate of current state changes of variables related to a system's physical current state (Goosse et al., 2010).

Mathematically, an abstract climate model is defined on function space X a dynamical system as

$$\frac{d(D\mathbf{u})}{dt} = A\mathbf{u} + N(\mathbf{u}) + F, \quad (3.4.1)$$

where \mathbf{u} is a vector of all predictive variable, D , A , and N change the number of grid cells and represent operators in X , and F represents climate forces (not include in \mathbf{u}). D is a linear operator, A is a linear operator with that has more complicated structure, and N is a nonlinear operator. (Goosse et al., 2010)

Then there are equations that describe the dynamics of what happens in the climate system, such as the **Clausius-Clapeyron equation** this equation related pressure to temperature is known as the pressure-temperature equation.

The intorpy S is function of temperature and volume $S(T, V)$ so the derivative dS is given by

$$dS = \left(\frac{\partial S}{\partial T} \right)_V dT + \left(\frac{\partial S}{\partial V} \right)_T dV, \quad (3.4.2)$$

at constant temperature and during phase change, the change in temperature is zero ($dT = 0$)then

$$dS = \left(\frac{\partial S}{\partial V} \right)_T dV, \quad (3.4.3)$$

this is lead us to 3rd Maxwell relations which is relation bettween dS and saturated P, T then

$$\left(\frac{\partial S}{\partial V} \right)_T = \left(\frac{\partial P}{\partial T} \right)_V, \quad (3.4.4)$$

from equation 3.4.3 we have

$$\left(\frac{\partial S}{\partial V} \right)_T = \frac{dS}{dV}, \quad (3.4.5)$$

then we can write

$$\left(\frac{\partial S}{\partial V}\right)_T = \left(\frac{dP}{dT}\right)_V = \frac{dS}{dV}, \quad (3.4.6)$$

so when we talk about two phases (gas and liquid) in equilibrium the values of saturated P and T will be independent of specific volume then we will have

$$\left(\frac{dP}{dT}\right)_{sat} = \frac{S_g - S_l}{V_g - V_l} = \frac{S_{lg}}{V_{lg}}, \quad (3.4.7)$$

where S_{lg} is entropy of vaporization and V_{lg} is the volume of vaporization then **Clausius-Clapeyron equation** as general expressions are

$$\frac{dP}{dT} = \frac{L_{lg}}{T V_{lg}} = \frac{\partial S}{\partial V}. \quad (3.4.8)$$

where L_{lg} the latent heat of the phase change.

Another is the **Stefan-Boltzmann Law** which describes the power emitted by a black body as a function of temperature, it is used in the thermal radiation equation.

$$P = \sigma \epsilon A T^4. \quad (3.4.9)$$

where P is the heat radiation power of the body, σ is the Stefan Boltzmann constant; ϵ is the emissivity of the substance, A is the surface area of the body, and T temperature of the body.

And **Navier-Stokes equation** also important for modelling dynamic flows in the atmosphere, the equation It represents fluid flow and it considers the heart of dynamic atmospheric flow modelling.

Three functions represent a fluid mathematically; density $\rho(x, t)$, pressure $p(x, t)$ and the velocity $u(x, t)$ are scalar functions of the position vector $\mathbf{x} = (x_1, x_2, x_3) \in \Gamma$ where Γ is a three-dimensional area filled with liquid.

The velocity of the fluid particle at point \mathbf{x} at time t and is given by the vector valued function $u(\mathbf{x}, t) = (u_1(\mathbf{x}, t), u_2(\mathbf{x}, t), u_3(\mathbf{x}, t))$. then the three functions ρ, p, u , governed by the momentum conservation equation described as

$$\rho \left(\frac{\partial u}{\partial t} + \sum_{i=1}^3 u_i \frac{\partial u}{\partial x_i} \right) - \mu \Delta u - (3\lambda + \mu) \nabla (\nabla \cdot u) + \nabla p = f, \quad (3.4.10)$$

this is the formula of Newton's second law of motion applicable to fluid mechanics. μ and λ are physical parameter and $f(x, t)$ is a force density per unit volume. The functions ρ, u, p also obey the continuity equation:

$$\frac{\partial \rho}{\partial t} + \nabla \cdot (\rho u) = 0, \quad (3.4.11)$$

If the fluid is homogeneous and incompressible then ρ is independent of the position and of the time then the equations 3.4.10 and 3.4.11 reduce to

$$\rho \left(\frac{\partial u}{\partial t} + \sum_{i=1}^3 u_i \frac{\partial u}{\partial x_i} \right) - \mu \nabla \cdot u + \nabla p = f, \quad (3.4.12)$$

$$\nabla \cdot u = 0, \quad (3.4.13)$$

we'll focus on the incompressible case below. The convention is to let $\rho = 1$, set $\mu = \nu$ (kinematic viscosity), then equation (3.4.12) will be

$$\frac{\partial u}{\partial t} + (u \cdot \nabla) u - \nu \Delta u + \nabla p = f, \quad (3.4.14)$$

The equation (3.4.13) together with (3.4.14) are the nondimensional incompressible NavierStokes equations, these equations are very important in fluid modelling, solving them for a particular set of boundary conditions predicts the fluid velocity and its pressure in a given geometry (Broomé and Ridenour, 2014).

Also we have the **conservation laws**, which are the laws that describe the behaviour and evolution of a model atmosphere. The model is given some variables for simulation, then the governing equations solve these variables or initial conditions to produce a new state of the atmosphere at a given time.

The set of seven equations with seven unknowns contains the density ,pressure ,specific humidity ,temperature and velocity (Three components (u, v, w)) ,the seven equations for the atmosphere are as follows:

Conservation of momentum (Newton's second law)

The equation obtaind from Newton's second law when the acceleration of air parcel moving in 3-dimensions is given by the physical forces per unit mass. Then we can express the acceleration by change in velocity per unit time to get:

$$\frac{d\vec{v}}{dt} = F/m \quad (3.4.15)$$

Then the complete Momentum Equation

$$\frac{d\vec{v}}{dt} = -\alpha \vec{\nabla} p - \vec{\nabla} \phi + \vec{F} - 2\Omega \times \vec{v} \quad (3.4.16)$$

Generally, there are three equations for three components of the velocity $\vec{v}(u, v, w)$, where \vec{F} is friction force and $\vec{\Omega}$ is angular velocity. The last term $(2\vec{\Omega} \times \vec{v})$ represents Coriolis force and ϕ is geopotential height. The equation relates the two apparent forces per unit mass (Coriolis and centrifugal on one side) to the real forces acting on a parcel of air such as the pressure gradient force, the gravitational force and the frictional force, on a rotating frame of reference.

Continuity equation

If we consider ρ is the fluid density then the vector mass flux will be $\rho\vec{v} = (\rho v, \rho u, \rho w)$. If mass of the air parcel is conserved, and at a local point there is divergence of the vector mass flux, then the density must decrease at that point. Let's assume a parcel having 3 infinitesimal dx, dy, dz then

$$\frac{d\rho}{dt} = \frac{\partial\rho}{\partial t} + \frac{\partial\rho}{\partial x}\frac{dx}{dt} + \frac{\partial\rho}{\partial y}\frac{dy}{dt} + \frac{\partial\rho}{\partial z}\frac{dz}{dt} \quad (3.4.17)$$

$$\frac{d\rho}{dt} = \frac{\partial\rho}{\partial t} + \frac{\partial\rho}{\partial x}u + \frac{\partial\rho}{\partial y}v + \frac{\partial\rho}{\partial z}w \quad (3.4.18)$$

$$\frac{d\rho}{dt} = \frac{\partial\rho}{\partial t} + \vec{\nabla} \cdot (\rho\vec{v}) \quad (3.4.19)$$

For incompressible fluids

$$\vec{\nabla} \cdot \vec{v} = 0 \quad (3.4.20)$$

This equation also known as mass conservation which is rate of increase of mass in fluid element equals the net rate of flow of mass into element delivered from a cubic. The equation usually referred to as flux form.

Equation of state for ideal gas

Nitrogen makes up 78.08 percent of the molecules in our atmosphere, whereas oxygen makes up 20.95 percent. Inert gases are also present in modest amounts. Ozone, a very significant stratospheric element, and carbon dioxide also exist in minor amounts that vary seasonally and over longer time intervals. They assume that these gaseous elements obey the ideal gas law, or that the atmosphere is assumed to be ideal gas in general :

$$P = \rho RT \quad (3.4.21)$$

This equation indicates that the given two thermodynamic variables, the others are determined, where ρ is density and R is the gas constant.

Conservation of energy equation The First Law of Thermodynamics state that the heat added or subtracted from the mass is the change in internal energy and the increment of work done on or by the air parcel.

$$dq = di + dw = C_p dT + gdz \quad (3.4.22)$$

Applying the hydrostatic approximation

$$\frac{dp}{dz} = -\rho g \quad (3.4.23)$$

Then

$$\frac{dq}{dt} = C_p \frac{dT}{dt} - \alpha \frac{dp}{dt} \quad (3.4.24)$$

Where $\frac{dq}{dt}$ represents the diabatic heating rate: all sources(surface sensible heating, elevated latent heating, or cloud-top radiative cooling) and the sinks of Energy. Then the complete Thermodynamic Energy Equation

$$C_p \left(\frac{\partial T}{\partial t} + \vec{v} \cdot \nabla T \right) = \frac{1}{\rho} \frac{dp}{dt} + Q + F_r \quad (3.4.25)$$

C_p is specific heat at constant volume, T is temperature and P pressure, .This law expresses the heat added or subtracted from the mass is the change in internal energy and the increment of work done on or by the air parcel.

Conservation equation for water mass (Moisture equation)

This equation describes the way in which the amount of water vapour in a particular parcel of air changes as result of advection and condensation C

$$\frac{\partial(\rho q)}{\partial t} = -\vec{\nabla} \cdot (\rho \vec{v} q) + \rho(E - C) \quad (3.4.26)$$

Where q is the water vapour mixing ratio and E is evaporation. The equation indicates that the total amount of water vapour in a parcel is conserved as the parcel moves around, except when there are sources such as evaporation and sinks

3.5 Model considered

The data used in this work to estimate the ToEs were generated by the MPI-ESM1-2-HR model that was released in 2017 from the Coupled Model Intercomparison Project 6th phase (CMIP6), which is a higher resolution version of the Max Planck Institute Earth System Model with a

horizontal resolution of $0.9^\circ \times 0.9^\circ$. The model run by the Max Planck Institute for Meteorology, Hamburg Germany in terms of native nominal Aerosol: 100 km, atmospheric: 100 km, land: 100 km, landIce: none, ocean: 50 km, ocnBgchem: 50 km, sealce: 50 km resolutions (von Storch et al., 2017).

MPI-ESM1-2-HR is based on historical climate simulations from 1850 to 2014, as well as future (2015-2100) conditions provided by bias adjustment and statistical downscaling of CMIP6 output. The model represents the global energy balance well and can reproduce the main patterns of atmospheric temperature, wind, precipitation, land surface air temperature, and sea surface temperature (SST) in a realistic manner (Wu et al., 2021)

3.6 Climate projection

Climate projection refers to long-term trends and projections that bear the imprint of climate change caused by both anthropic and natural climate forces. Mathematically, it is expressed as

$$\text{Climate projection} = \left[\frac{F - R}{R} \right] \times 100. \quad (3.6.1)$$

Where F represents future values and R represents reference values. This equation is used to calculate the percentage increase or decrease in the projected change in precipitation indicators (Collins et al., 2013).

3.7 Estimating the Time of Emergence (ToE)

Estimating ToEs of the change in precipitation signal requires estimates of both the precipitation signal and the normal variation or noise. This leads us to choose the signal-to-noise ratio method that defines the ToE as the first year that the signal-to-noise ratio surpass a certain sill established in advance (Hawkins and Sutton, 2012).

This method defines the noise as the standard deviation of annual or seasonal mean precipitation. For noise estimation, we used data from the MPI-ESM1-2-HR simulation covering the whole region for the period 1950 to 2100. The period is a combination of historical experimentation and future scenarios (both contain natural fluctuations). Note that this choice is consistent with many previous studies including Hawkins and Sutton (2012), (Giorgi and Bi, 2009) and Gaetani et al. (2020). The noise can be defined mathematically as :

$$\text{Noise} = \sqrt{\frac{\sum_{i=1}^N (x_i - \bar{x})^2}{N}}, \quad (3.7.1)$$

where N is the size of the population, x_i is each value from the population and \bar{x} is the population mean. The simulation from the model should estimate the natural variability (change in climate parameters) in the absence of human influence. This noise (standard deviation) should be a function of latitude and longitude. And it should be computed for both historical and future scenarios.

While the signal $S(t)$ was estimated from simple linear regression, we use data from 1950–2099 from MPI-ESM1-2-HR simulation. First we create a smoothed average second order polynomial, fitted over the period 1950–2099 ([Hawkins and Sutton, 2012](#)) for our data, because values that are close in time are likely to be close in value as well.

Then a simple linear regression model was applied to regress the precipitation at each grid point. The regression is supposed to estimate the precipitation at each grid point and it can be expressed mathematically as:

$$\mathbf{y} = \beta_1 X + \beta_0. \quad (3.7.2)$$

For better estimation of the regression coefficients (β_0, β_1) in Equation 3.7.2, Ordinary Least Squares regression (OLS) was used. The theoretical regression model can be expressed as:

$$\mathbf{y}_i = \beta_0 + \beta_1 X_i + \epsilon_i, \quad (3.7.3)$$

We want to find an estimated regression line

$$\hat{\mathbf{y}}_i = \hat{\beta}_0 + \hat{\beta}_1 X_i, \quad (3.7.4)$$

where $\hat{\beta}_0$ and $\hat{\beta}_1$ are regression coefficients estimated by minimizing the sum squared of error.

$$\sum_{i=1}^n \epsilon_i^2 = \sum_{i=1}^n (\mathbf{y}_i - \hat{\mathbf{y}}_i)^2 = \sum_{i=1}^n (\mathbf{y}_i - (\hat{\beta}_0 + \hat{\beta}_1 X_i))^2. \quad (3.7.5)$$

taking the partial derivative with respect to $\hat{\beta}_0$

$$\frac{\partial}{\partial \hat{\beta}_0} \sum_{i=1}^n (\mathbf{y}_i - (\hat{\beta}_0 + \hat{\beta}_1 X_i))^2 = \sum_{i=1}^n \frac{\partial}{\partial \hat{\beta}_0} (\mathbf{y}_i - (\hat{\beta}_0 + \hat{\beta}_1 X_i))^2, \quad (3.7.6)$$

$$= -2 \sum_{i=1}^n (\mathbf{y}_i - (\hat{\beta}_0 + \hat{\beta}_1 X_i)), \quad (3.7.7)$$

and the derivative with regard to $\hat{\beta}_1$

$$\frac{\partial}{\partial \hat{\beta}_1} \sum_{i=1}^n (\mathbf{y}_i - (\hat{\beta}_0 + \hat{\beta}_1 X_i))^2 = \sum_{i=1}^n \frac{\partial}{\partial \hat{\beta}_1} (\mathbf{y}_i - (\hat{\beta}_0 + \hat{\beta}_1 X_i))^2, \quad (3.7.8)$$

$$= -2 \sum_{i=1}^n X_i (\mathbf{y}_i - (\hat{\beta}_0 + \hat{\beta}_1 X_i)), \quad (3.7.9)$$

then setting the partial derivatives equal to zero

$$-2 \sum_{i=1}^n (\mathbf{y}_i - (\hat{\beta}_0 + \hat{\beta}_1 X_i)) = 0, \quad (3.7.10)$$

$$-2 \sum_{i=1}^n X_i (\mathbf{y}_i - (\hat{\beta}_0 + \hat{\beta}_1 X_i)) = 0, \quad (3.7.11)$$

and solving for $\hat{\beta}_0$

$$\sum_{i=1}^n (\mathbf{y}_i - (\hat{\beta}_0 + \hat{\beta}_1 X_i)) = \sum_{i=1}^n \mathbf{y}_i - \sum_{i=1}^n \hat{\beta}_0 - \sum_{i=1}^n \hat{\beta}_1 X_i = 0, \quad (3.7.12)$$

which lead to

$$\sum_{i=1}^n \mathbf{y}_i - n \hat{\beta}_0 - \sum_{i=1}^n \hat{\beta}_1 X_i = 0, \quad (3.7.13)$$

and

$$\hat{\beta}_0 = \frac{1}{n} \left(\sum_{i=1}^n \mathbf{y}_i - \hat{\beta}_1 \sum_{i=1}^n X_i \right). \quad (3.7.14)$$

$$\hat{\beta}_0 = \bar{\mathbf{y}} - \hat{\beta}_1 \bar{\mathbf{X}}. \quad (3.7.15)$$

Now let's solve for $\hat{\beta}_1$:

Firstly, we start by taking the derivative with respect to $\hat{\beta}_1$

$$\frac{\partial}{\partial \hat{\beta}_1} \sum_{i=1}^n (\mathbf{y}_i - (\hat{\beta}_0 + \hat{\beta}_1 X_i))^2 = \sum_{i=1}^n \frac{\partial}{\partial \hat{\beta}_1} (\mathbf{y}_i - (\hat{\beta}_0 + \hat{\beta}_1 X_i))^2, \quad (3.7.16)$$

$$= -2 \sum_{i=1}^n X_i (\mathbf{y}_i - (\hat{\beta}_0 + \hat{\beta}_1 X_i)), \quad (3.7.17)$$

then setting the partial derivatives equal to zero

$$\sum_{i=1}^n X_i(\mathbf{y}_i - (\hat{\beta}_0 + \hat{\beta}_1 X_i)) = 0, \quad (3.7.18)$$

By substituting β_0 from equation 3.7.15

$$\sum_{i=1}^n X_i(\mathbf{y}_i - (\bar{\mathbf{y}} - \underbrace{\hat{\beta}_1 \bar{X}}_{\beta_0} + \hat{\beta}_1 X_i)) = 0. \quad (3.7.19)$$

$$\sum_{i=1}^n X_i(\mathbf{y}_i - \bar{\mathbf{y}}) - \hat{\beta}_1 X_i(\bar{X} - X_i) = 0, \quad (3.7.20)$$

Then we can separate the equation as

$$\sum_{i=1}^n X_i(\mathbf{y}_i - \bar{\mathbf{y}}) = \hat{\beta}_1 \sum_{i=1}^n X_i(\bar{X} - X_i), \quad (3.7.21)$$

Then

$$\hat{\beta}_1 = \frac{\sum_{i=1}^n X_i(\mathbf{y}_i - \bar{\mathbf{y}})}{\sum_{i=1}^n X_i(\bar{X} - X_i)} \quad (3.7.22)$$

Note

$$\sum_{i=1}^n (X_i - \bar{X})(\mathbf{y}_i - \bar{\mathbf{y}}) = X_i \sum_{i=1}^n (\mathbf{y}_i - \bar{\mathbf{y}}) - \bar{X} \sum_{i=1}^n (\mathbf{y}_i - \bar{\mathbf{y}}) \underbrace{\quad}_{0} \quad (3.7.23)$$

$$= \sum_{i=1}^n X_i(\mathbf{y}_i - \bar{\mathbf{y}}), \quad (3.7.24)$$

and

$$\sum_{i=1}^n (X_i - \bar{X})^2 = \sum_{i=1}^n (X_i - \bar{X})(X_i - \bar{X}) \quad (3.7.25)$$

$$= \sum_{i=1}^n X_i(X_i - \bar{X}) - \bar{X} \sum_{i=1}^n (X_i - \bar{X}) \underbrace{\quad}_{0} \quad (3.7.26)$$

$$= \sum_{i=1}^n X_i(X_i - \bar{X}), \quad (3.7.27)$$

then equation 3.7.22 can be written as :

$$\hat{\beta}_1 = \frac{\sum_{i=1}^n (X_i - \bar{X})(y_i - \bar{y})}{\sum_{i=1}^n (X_i - \bar{X})^2} \quad (3.7.28)$$

then the following expressions are obtained by solving the minimization problem:

$$\hat{\beta}_1 = \frac{\sum_{i=1}^n (X_i - \bar{X})(y_i - \bar{y}_i)}{\sum_{i=1}^n (X_i - \bar{X})^2} = \frac{\sum_{i=1}^n X_i y_i - n \bar{X} \bar{y}}{X^2 - n \bar{X}^2}, \quad (3.7.29)$$

$$\hat{\beta}_0 = \bar{y} - \hat{\beta}_1 \bar{X}, \quad (3.7.30)$$

Therefore, the signal $S(t)$ can be expressed as mathematically as

$$S(t) = \beta_1 X(t) + \beta_0. \quad (3.7.31)$$

Now we generate the time-dependent signal S and use it to predict a precipitation time series at each grid point, saving in a netCDF format with three-dimensional (longitude,latitude,time). Then we compare this estimate to the noise, and we determine the time at which the ratio $(\frac{S(t)}{N})$ exceeds some threshold we set (it's our time of emergence) to obtain the ToEs.

The flow chart in Figure 3.3 summarize the methodological approach

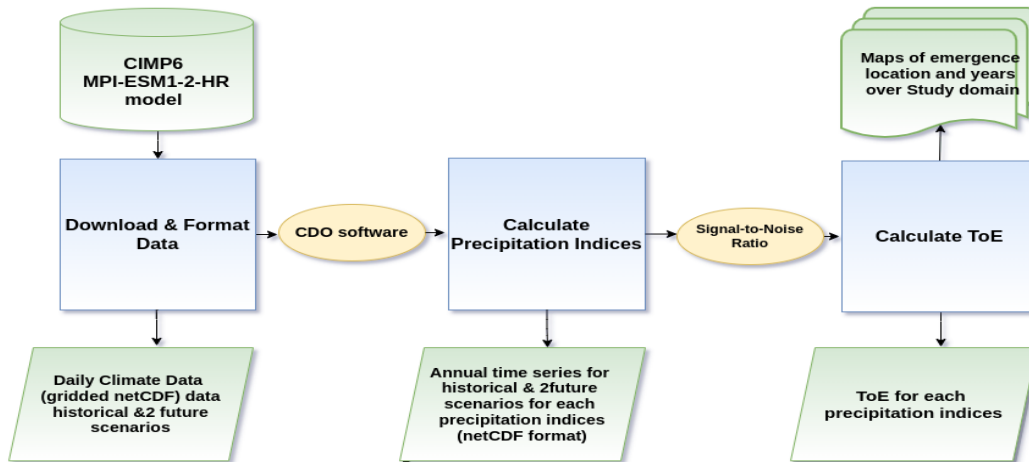


Figure 3.3: Flow chart indicating data sources, steps, and outputs for ToE.

4. Result and Discussion

This chapter is divided into two sections that discuss the findings of our study. The first section shows the projected change in precipitation indices, looks the rate of precipitation change between the near and far future. In the second section, the time of emergence for each precipitation indices is shown, along with a comparison of future scenarios output.

ToE is estimated for three precipitation indices: the frequency of wet days, the annual mean precipitation and number of heavy precipitation days (greater than 10 mm). This is done separately for each future scenario. This study classifies early ToE up to 2040, mid ToE the period 2040–2080 and late ToE beyond 2080 ([Nguyen et al., 2018a](#)).

4.1 Projected change in the frequency of wet days

The frequency of wet days index is defined as the frequency of days when precipitation is greater than one millimetre. The spatial distribution maps presented in Figure [4.1](#) depict the projected change of frequency of wet days in both Sudan and South Sudan. The maps are based on referenced and assimilated data obtained from the MPI-ESM1-2-HR model, which was integrated for two future scenarios (SSP2-4.5 and SSP5-8.5). Each scenario is split into two periods. The period from 2031 to 2060 is referred to as the near future, while the period from 2070 to 2099 is referred to as the far future.

The colour bar in Figure [4.1](#) shows the frequency of wet days in percentage increase and decrease change, which ranges from -100% to $+100\%$. It can be observed in all maps, representing the far and near future of both scenarios, that there exists a high percentage decrease change in the frequency of wet days at rate of -75% in northern Sudan. This denotes aridity and infrequent precipitation in this region, which represents the Sahara desert. The center area has experienced a significant increase in the number of wet days up to 70% ; this area is semi-arid and contains several plateaus and mountains, which explains the region's higher precipitation than the northern parts. We may also see a progressive increase towards the south.

Whereas, the percentage increase and decrease change in the frequency of wet days in South Sudan, in the same scenario mentioned above it ranges between -25% and 25% . This indicates a small change in the frequency of wet days in the country, except for the far future of SSP5-8.5 show more increase of the rate of change up to 50% .

There is substantial evidence to support a shift in the overall precipitation patterns in Sudan during this period. The results show a high decrease in the frequency of wet days in north Sudan and a high increase in the south part. This result is consistent with results of [Shongwe et al. \(2011\)](#). This result show a slight change in the frequency of wet days South Sudan, which is consistent with the results of [Colin Quinn and Habib \(2019\)](#)

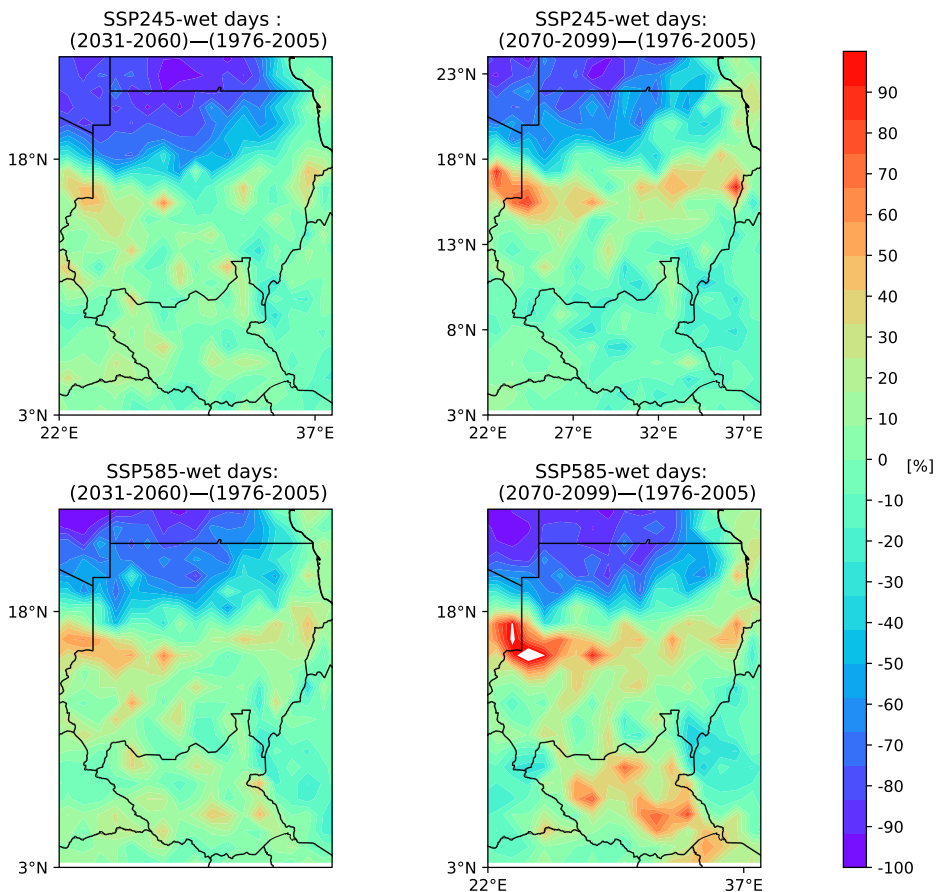


Figure 4.1: Projected change in the frequency of wet days in Sudan and South Sudan

4.2 The ToE of change in the frequency of wet days

The ToE of the change in the frequency of wet days is defined as the time when the frequency of wet days begins to change from what it had been in the past variability. Figure 4.2 shows the ToE of the change in the frequency of wet days over Sudan and South Sudan, using MPI-ESM1-2-HR historical and future scenarios. The figure also shows two different ratios (1 and 2) for both of the scenarios.

The ToE of the change in the frequency of wet days precipitation index was examined using the signal-to-noise ratio method, and years that exceeded the threshold (1 and 2) were considered. For the ratio 1, the assessment shows the late emergence of ToE in north Sudan within the last two decades of the twenty-first century, later than 2080. In fact, the late emergence in the frequency of wet days in the north of Sudan is due to scarcity of the precipitation in this region, which is the Sahra desert. These desert regions are characterized by the reduced occurrence of wet days (as shown in Figure 4.1). Ratio 2 shows the early emergence of the frequency of wet days in some locations. For many regions in central Sudan, ToE assessment shows early emergence within the next two decades, before 2040 for both ratios.

In South Sudan, the results showed early emergence in ToE of the change in frequency of wet days within the first two decades of the twenty-first century before 2020. With the exception in the second scenario (SSP5-8.5) for some locations where the frequency of wet days is occurring in the current decade. The purple colour (below year 2000) indicates that the change in the frequency of wet days already occurs from natural variability at this location during this period.

Sudan is characterized by variation in the climate conditions and topography between its different regions. As a result, the intriguing discrepancy in the ToE in the frequency of wet days between its various areas can be explained. Whereas the ToE results of the change in the frequency of wet days in South Sudan show in the early twenty-first century. This result is consistent with [Giorgi and Bi \(2009\)](#)

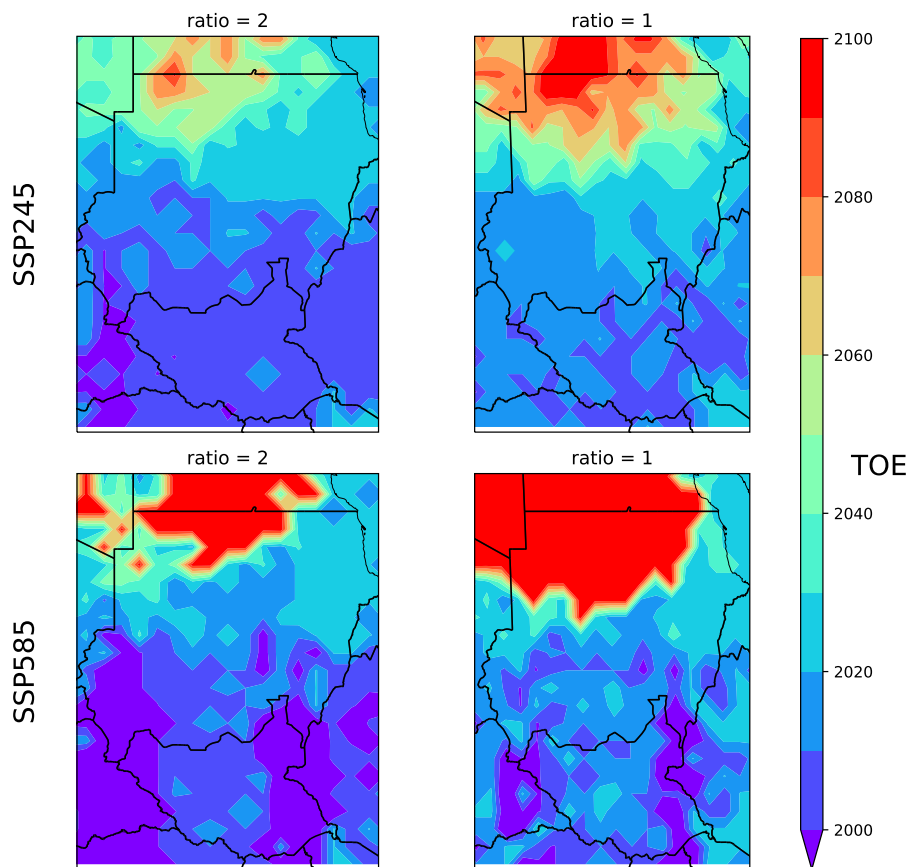


Figure 4.2: The ToE of change in the frequency of wet days in Sudan and South Sudan

4.3 Projected change in the annual mean precipitation

The annual mean precipitation is defined as the amount of precipitation expected in a given area per year. The spatial distribution maps presented in Figure 4.3 depicts the projected change of the annual mean precipitation in both Sudan and South Sudan. The maps are based on referenced and assimilated data obtained from the MPI-ESM1-2-HR, which was integrated from two future

scenarios. The colour bar in Figure 4.3 indicates a positive sign for rising values and a negative sign for declining values. It can be observed that the change in annual mean precipitation in Sudan is increasing at a rate of more than 75 % in the semi-arid areas. This result is consistent with the results of Rhodes (2012). And gradually decreasing towards the south up to reach -10 %.

We observed a slight change in the rate of change in annual mean precipitation in South Sudan. The overall result shows an increase in annual mean precipitation at a rate of less than 30% in the near future and decreases at a rate of -10 %.

The greatest increase was under the most severe emission scenario of SSP5-8.5 in the far future, up to 90% in Sudan and 70% in South Sudan.

The north of Sudan appears to be suffering from a lack of precipitation, with white areas indicating that the change cannot be assessed in these areas; this could be due to the region's lack of precipitation, which represents the Sahara desert. Whereas the results of South Sudan showed a slight change in the annual mean precipitation, which is close to the result of the change in the frequency of wet days (shown in Figure 4.1). This indicates that the projected change in the precipitation in South Sudan is slight during the 21st century which makes this result consistent with the results of Colin Quinn and Habib (2019) and Rhodes (2012).

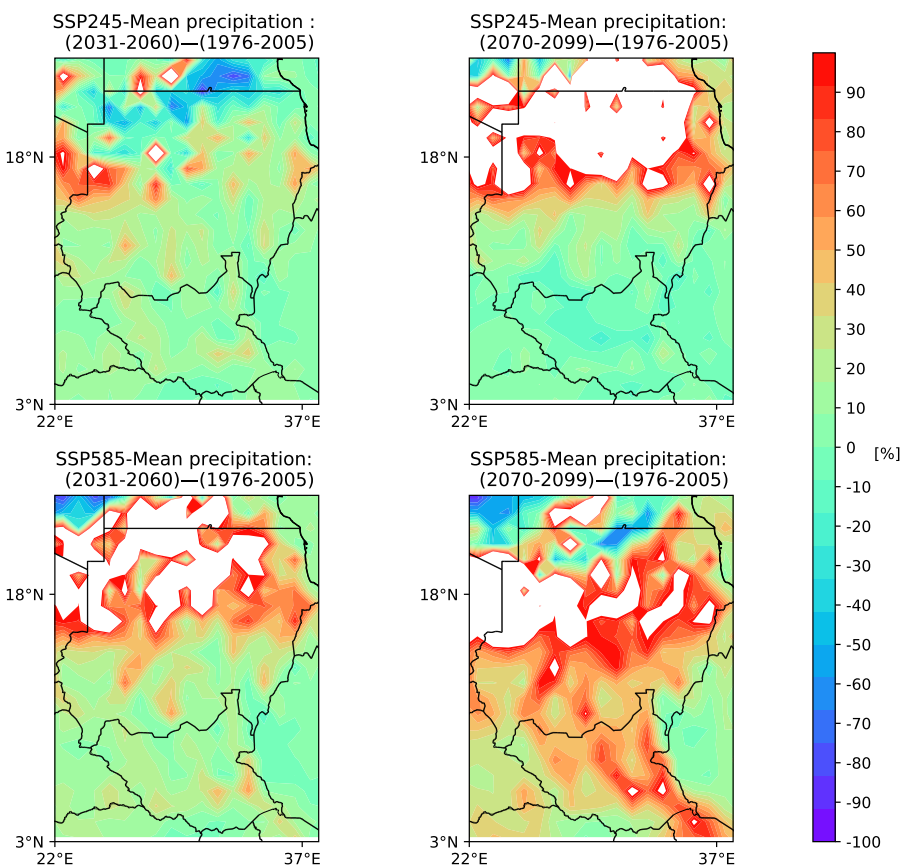


Figure 4.3: Projected changes of annual mean precipitation in Sudan and South Sudan

4.4 The ToE of the change in the annual mean precipitation

The ToE of the change in the annual mean precipitation is the time when the annual mean precipitation begins to change from what it had been in the prior variability. Figure 4.3 shows the ToE of the change in the annual mean precipitation over Sudan and South Sudan using MPI-ESM1-2-HR historical and future scenarios.

ToE assessment for the change in the annual mean precipitation shows early emergence in Sudan, over the next two decades of the twenty-first century before 2040. ToE was detected in many locations in central and southern Sudan before 2020 for both ratios. The northern parts show the ToE will be within the 2030s. The purple colour that is covering parts from south Sudan in the ratio 2 indicates that the change occurred from natural variability.

In South Sudan, the results show early emergence in ratio 1, and it will be within the first years of the 21st century for some locations. where, ratio 2 indicates that the change in the annual mean precipitation already occurs from natural variability in the 20st century. The ToEs of the change in precipitation in tropical regions appear to be due to natural variability or early in the twenty-first century.

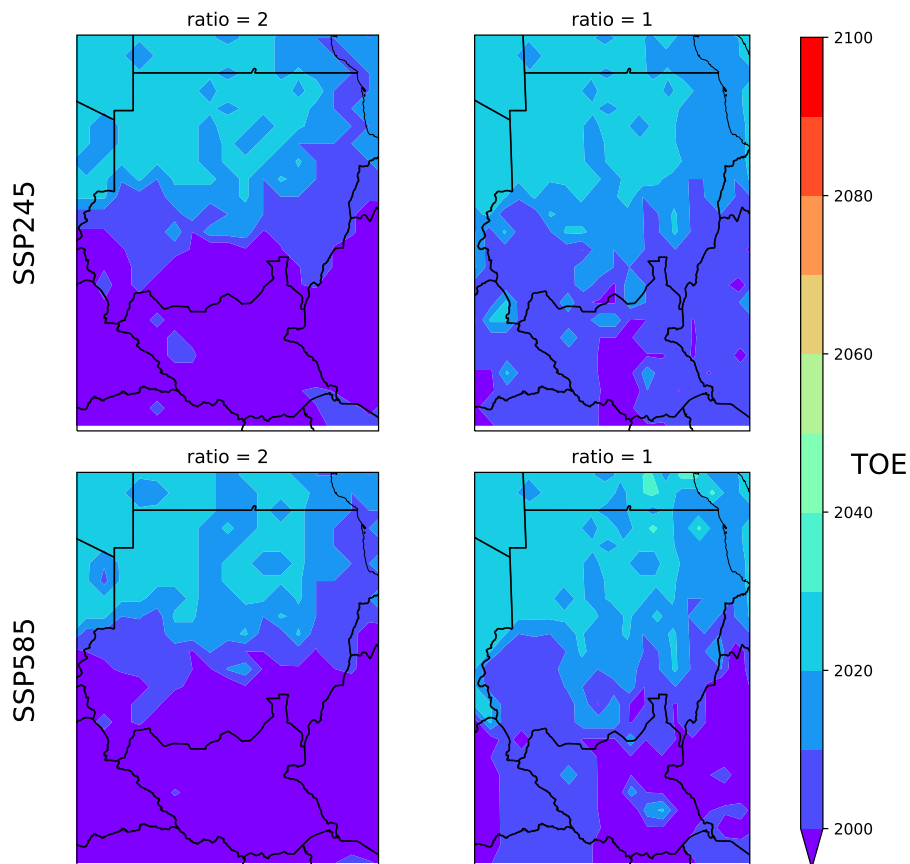


Figure 4.4: The ToE of the change in the annual mean precipitation

As evidenced by the frequency of wet days and mean precipitation. In fact, this finding is consistent with the majority of studies, including Nguyen et al. (2018a) .

4.5 Projected change in the number of heavy precipitation days

The annual heavy day's precipitation is defined as the count of days with precipitation greater than 10 millimetres. Figure 4.5 depicts the overall projected changes in heavy precipitation days over Sudan and South Sudan. We can see that the projected change in 4.5 is similar in some ways to the projected change in the frequency of wet days in Figure 4.1.

The colour bar in Figure 4.5 depicts the percentage increase and decrease change in heavy precipitation days. Heavy precipitation days are projected to decline significantly in north Sudan under SSP2–4.5 and SSP5–8.5 scenarios. The rate of decreasing change reaches -100 % in some locations. This significant reduction in the rate of change in the number of heavy precipitation days is because of the rare precipitation in this region.

Many central regions can be observed to have experienced a significant increase in the rate of change of the annual heavy precipitation days reaching up to 60 % and decreasing gradually up to reach -10 %. In fact, this is semi-arid regions are characterised by an increase in the occurrence of heavy precipitation days in comparison with north parts.

In contrast, in the same scenario, the percentage increase and decrease change in the number of heavy precipitation days over South Sudan reaches up to 60%and gradually decreases to -10%.

The large decrease and increase in the change of heavy precipitation days is shown in SSP5–8.5, which shows an increase in the rate of change of up to more than 80% in South Sudan and 70%in Sudan. Furthermore, we can see from all of the maps that there is no decrease in the change in South Sudan, indicating an increase in the occurrence of heavy precipitation days. In contrast, Sudan has a different percentage change across the different country's regions. Where the northern part is suffering from hard drier and receives a small amount of precipitation. where the precipitation decreases towards the semi-arid region that has water strain somehow small in comparison with the northern parts.

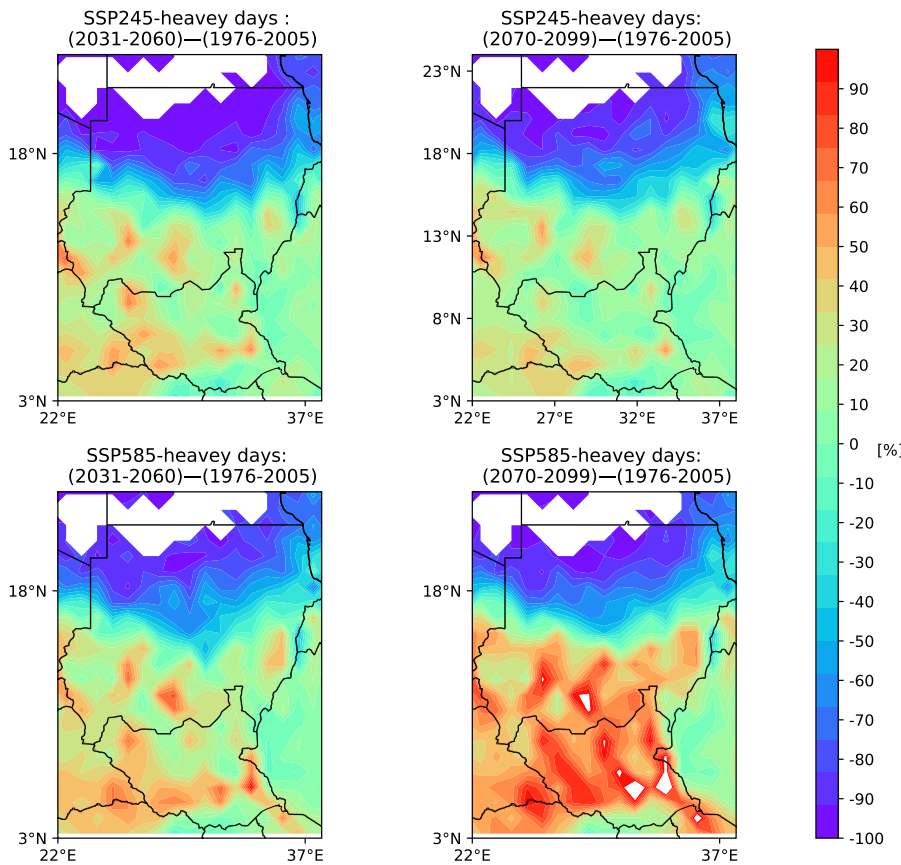


Figure 4.5: Projected change in the number of heavy precipitation days in Sudan and South Sudan

4.6 The ToE of the change in the number of heavy precipitation days

The ToE of the change in the number of heavy precipitation days is the time when the number of heavy precipitation days start to change from what it had been in the porir variability.

Figure 4.6 shows the ToE of the change in the number of heavy precipitation days over Sudan and South Sudan by using MPI-ESM1-2-HR historical and future scenarios. ToE analysis of the change in the number of heavy precipitation days shows an early emergence in the north and central Sudan over the next two decades of the twenty-first century, before 2040. In southern parts of Sudan, it can be observed that the ToEs have already occurred from natural variability within the 20th century. With the exception of SSP5-8.5 for ratio 1, it shows early emergence in some locations in the south.

In South Sudan, the results show that the ToE of the change in the number of heavy precipitation days occurs naturally in the twentieth century. The strongest emission scenario of SSP5-8.5, on the other hand, shows an early emergence of the change in the number of heavy precipitation

days in the ratio 1.

The results showed that Sudan is a country that is extremely vulnerable to climate change. ToEs of the change in precipitation is vary across the country's regions, from the north to the south. Whereas South Sudan, is less vulnerable to climate change in comparison with Sudan.

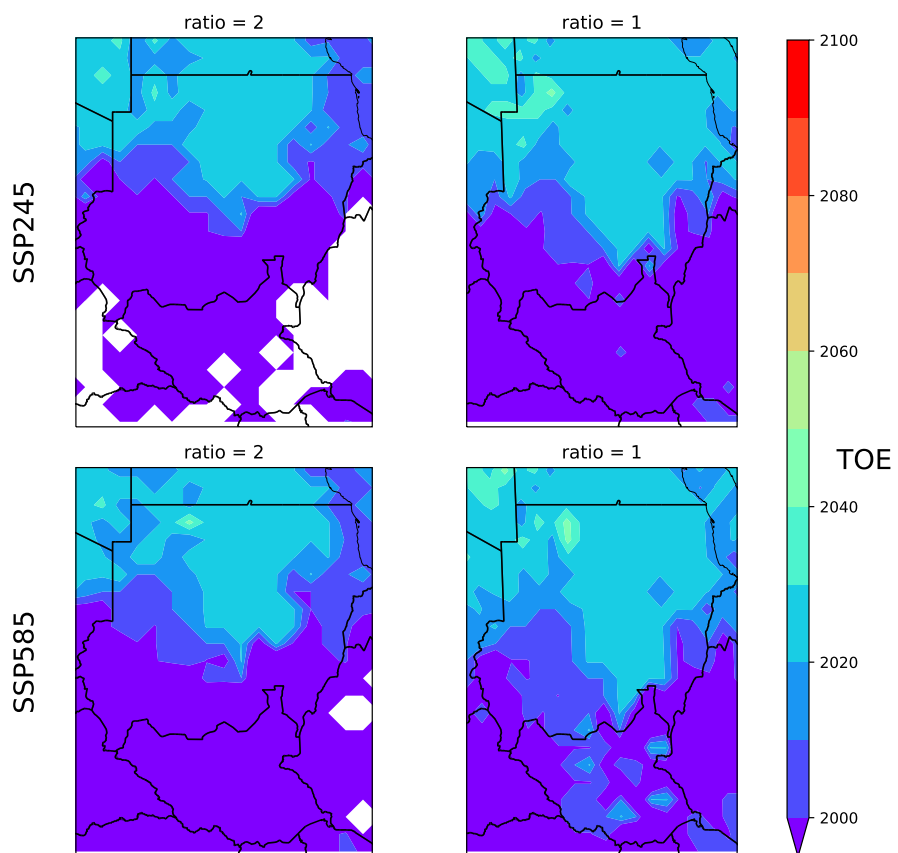


Figure 4.6: Time of Emergence of the heavy days precipitation

5. Conclusion

In this research, we used a signal-to-noise ratio method to estimate the Time of Emergence (ToE) of the change in precipitation over Sudan and South Sudan during the twenty-first century using CMIP6 multimodel datasets simulated under SSPs scenarios. We investigated the projected change and ToEs of the change in precipitation by examining three precipitation indices: the frequency of wet days, the annual mean precipitation and the annual number of heavy precipitation days. We observed that all the indices exhibited a significant decreasing rate that can reach, up to 100% in northern Sudan, with a gradual increase towards the south. South Sudan, on the other hand, showed a slight change in the projected change in precipitation when compared to Sudan. Among all the indices, the ssp5-8.5 indicated the greatest increase in the distant future.

ToE assessment showed a late emergence in the frequency of wet days within the last two decades of the twenty-first century after 2080, whereas ToE of the annual mean precipitation and number of heavy precipitation days within the next two decades of the twenty-first century before 2040 in the north of Sudan. whereas, for many central Sudanese regions, the early emergence of ToEs before 2040 is expected.

However, in South Sudan, ToEs of change in the annual mean precipitation and the frequency of wet days occur early within the twenty-first century before 2020. ToE assessment of a number of heavy precipitation days revealed already occurs from natural variability in the Twentieth century. Furthermore, we note that the SSP2-4.5 scenario showed an early emergence for ToEs than the SSP5-8.5 scenario.

References

- Alan Beardon. From Problem Solving to Research, 2006. Unpublished manuscript.
- Sofia Broomé and Jonathan Ridenour. A pde perspective on climate modeling, 2014.
- Cristián Chadwick, Jorge Gironás, Sebastián Vicuña, and Francisco Meza. Estimating the local time of emergence of climatic variables using an unbiased mapping of GCMs: An application in semiarid and Mediterranean Chile. *Journal of Hydrometeorology*, 20(8):1635–1647, 2019.
- Intergovernmental Panel On Climate Change. Ipcc. *Climate change*, 2014.
- Climate Change Knowledge Portal. Climate change knowledge portal. <https://climateknowledgeportal.worldbank.org/>.
- Climate Change Knowledge Portal. "Climate Change Knowledge Portal For Development Practitioners Policy Makers", 2022. URL <https://climateknowledgeportal.worldbank.org/country/>. [Online; accessed 17-MAY-2022].
- Kye Baroang Dan Evans Melq Gomes Colin Quinn, Ashley Fox and Josh Habib, 2019.
- Matthew Collins, Reto Knutti, Julie Arblaster, Jean-Louis Dufresne, Thierry Fichefet, Pierre Friedlingstein, Xuejie Gao, William J Gutowski, Tim Johns, Gerhard Krinner, et al. Long-term climate change: projections, commitments and irreversibility. In *Climate Change 2013-The Physical Science Basis: Contribution of Working Group I to the Fifth Assessment Report of the Intergovernmental Panel on Climate Change*, pages 1029–1136. Cambridge University Press, 2013.
- Countries of the World and Their Leaders Yearbook . "Countries of the World and Their Leaders Yearbook ", 2022. URL <https://www.encyclopedia.com/international/culture-magazines/sudan>. [Online; accessed 12-April-2022].
- Ahmed H Elfaig, Ibrahim M Eltom, and Abdelrahim Salih. Rainfall Variability in the Sahel: A study from Sudan (1970-2010). 2013.
- Veronika Eyring, Sandrine Bony, Gerald A Meehl, Catherine A Senior, Bjorn Stevens, Ronald J Stouffer, and Karl E Taylor. Overview of the Coupled Model Intercomparison Project Phase 6 (CMIP6) experimental design and organization. *Geoscientific Model Development*, 9(5): 1937–1958, 2016.
- Nihal Fernando and Walter Garvey. Republic of South Sudan: The Rapid Water Sector Needs Assessment and a Way Forward. 2013.
- Marco Gaetani, Serge Janicot, Mathieu Vrac, Adjoua Moise Famien, and Benjamin Sultan. Robust assessment of the time of emergence of precipitation change in West Africa. *Scientific reports*, 10(1):1–10, 2020.
- Filippo Giorgi and Xunqiang Bi. Time of emergence (TOE) of GHG-forced precipitation change hot-spots. *Geophysical Research Letters*, 36(6), 2009.

- Hugues Goosse, Pierre-Yves BARRIAT, Marie-France LOUTRE, and Violette ZUNZ. *Introduction to climate dynamics and climate modeling*. Centre de recherche sur la Terre et le climat Georges Lemaître-UCLouvain, 2010.
- Ed Hawkins and Rowan Sutton. Time of emergence of climate signals. *Geophysical Research Letters*, 39(1), 2012.
- <https://cordex.org/about/>. WCRP Coordinated Regional Climate Downscaling Experiment. Accessed:2022 -04-16.
- J Hurrell, M Visbeck, and P Pirani. WCRP coupled model intercomparison project-phase 5-CMIP5. *Clivar Exchanges*, 16(56):1–52, 2011.
- IFRC. Sudan: Floods, 2010.
- Eun-Soon Im, Nguyen-Xuan Thanh, Liying Qiu, Moetasim Ashfaq, Xuejie Gao, Tong Yao, Csaba Torma, Mojisola O Adeniyi, Sushant Das, Graziano Giuliani, et al. Emergence of robust anthropogenic increase of heat stress-related variables projected from CORDEX-CORE climate simulations. *Climate Dynamics*, 57(5):1629–1644, 2021.
- Julio V Iribarne and Warren Lehman Godson. *Atmospheric thermodynamics*, volume 6. Springer Science & Business Media, 1981.
- Eugenia Kalnay. *Atmospheric modeling, data assimilation and predictability*. Cambridge university press, 2004.
- Manfred Wiebelt Tingju Zhu Khalid Siddig, Davit Stepanyan and Harald Grethe, editors. *Climate Change and Agriculture in the Sudan*. 2018.
- Kewei Lyu, Xuebin Zhang, John A Church, Aimee Slanger, and Jianyu Hu. Time of emergence for regional sea-level change. *Nature Climate Change*, 4(11):1006–1010, 2014.
- D. J. C. MacKay and R. M. Neal. Good codes based on very sparse matrices. Available from www.inference.phy.cam.ac.uk, 1995.
- David MacKay. "Statistical Testing of High Precision Digitisers". Technical Report 3971, Royal Signals and Radar Establishment, Malvern, Worcester. WR14 3PS, 1986.
- Mankin Mak. *Atmospheric dynamics*. Cambridge University Press, 2011.
- Matthew Davey. *Error-correction using Low-Density Parity-Check Codes*. Phd, University of Cambridge, 1999.
- GABRIELS Donald Maurice. College on Soil Physics-30th Anniversary (1983-2013). 2013.
- Mostafa A Mohamed and Mohamed El-Sayed El-Mahdy. Impact of sunspot activity on the rainfall patterns over Eastern Africa: a case study of Sudan and South Sudan. *Journal of Water and Climate Change*, 12(5):2104–2124, 2021.

- Thuy-Huong Nguyen, Seung-Ki Min, Seungmok Paik, and Donghyun Lee. Time of emergence in regional precipitation changes: an updated assessment using the CMIP5 multi-model ensemble. *Climate Dynamics*, 51(9):3179–3193, 2018a.
- Thuy-Huong Nguyen, Seung-Ki Min, Seungmok Paik, and Donghyun Lee. Time of emergence in regional precipitation changes: an updated assessment using the CMIP5 multi-model ensemble. *Climate Dynamics*, 51(9):3179–3193, 2018b.
- Mutasim Bashir Nimir and Ismail Elgizouli. Climate Change Adaptation and Decision Making in the Sudan. *World Resources Institute*. <https://www.wri.org/our-work/project/world-resources-report/climate-change-adaptation-and-decision-making-sudan>, 2013.
- Oxford University . "Oxford Languages", 2019. URL <https://languages.oup.com/word-of-the-year/2019/>. [Online; accessed 26-May-2022].
- World Food Programme. Food Security and Climate Change Assessment: Sudan, 2016.
- Gandomè Mayeul Léger Davy Quenum, Francis Nkrumah, Nana Ama Browne Klutse, and Mouhamadou Bamba Sylla. Spatiotemporal Changes in Temperature and Precipitation in West Africa. Part I: Analysis with the CMIP6 Historical Dataset. *Water*, 13(24):3506, 2021.
- R Rhodes. Changes in long-term variability of the rains of Sudan. *M. Sc. Dissertation*, 2012.
- Keywan Riahi, Detlef P Van Vuuren, Elmar Kriegler, Jae Edmonds, Brian C O'Neill, Shinichiro Fujimori, Nico Bauer, Katherine Calvin, Rob Dellink, Oliver Fricko, et al. The shared socioeconomic pathways and their energy, land use, and greenhouse gas emissions implications: an overview. *Global environmental change*, 42:153–168, 2017.
- Sarah Schlunegger, Keith B Rodgers, Jorge L Sarmiento, Tatiana Ilyina, John P Dunne, Yohei Takano, James R Christian, Matthew C Long, Thomas L Frölicher, Richard Slater, et al. Time of emergence and large ensemble intercomparison for ocean biogeochemical trends. *Global biogeochemical cycles*, 34(8):e2019GB006453, 2020.
- Claude Shannon. "A Mathematical Theory of Communication". *Bell Sys. Tech. J.*, 27:379–423, 623–656, 1948.
- Claude Shannon. The Best Detection of Pulses. In N. J. A. Sloane and A. D. Wyner, editors, *Collected Papers of Claude Shannon*, pages 148–150. IEEE Press, New York, 1993.
- Mxolisi E Shongwe, Geert Jan van Oldenborgh, Bart Van den Hurk, and Maarten van Aalst. Projected changes in mean and extreme precipitation in Africa under global warming. Part II: East Africa. *Journal of climate*, 24(14):3718–3733, 2011.
- Bharat Raj Singh and Onkar Singh. Study of impacts of global warming on climate change: rise in sea level and disaster frequency. *Global warming—impacts and future perspective*, 2012.
- Yue Sui, Xianmei Lang, and Dabang Jiang. Time of emergence of climate signals over China under the RCP4.5 scenario. *Climatic change*, 125(2):265–276, 2014.

Hyun Min Sung, Jisun Kim, Sungbo Shim, Jeong-byun Seo, Sang-Hoon Kwon, Min-Ah Sun, Hyejin Moon, Jae-Hee Lee, Yoon-Jin Lim, Kyung-On Boo, et al. Climate change projection in the twenty-first century simulated by NIMS-KMA CMIP6 model based on new GHGs concentration pathways. *Asia-Pacific Journal of Atmospheric Sciences*, 57(4):851–862, 2021.

Jin-Song von Storch, Dian Putrasahan, Katja Lohmann, Oliver Gutjahr, Johann Jungclaus, Matthias Bittner, Helmuth Haak, Karl-Hermann Wieners, Marco Giorgetta, Christian Reick, Monika Esch, Veronika Gayler, Philipp de Vrese, Thomas Raddatz, Thorsten Mauritsen, Jörg Behrens, Victor Brovkin, Martin Claussen, Traute Crueger, Irina Fast, Stephanie Fiedler, Stefan Hagemann, Cathy Hohenegger, Thomas Jahns, Silvia Kloster, Stefan Kinne, Gitta Lasslop, Luis Kornblueh, Jochem Marotzke, Daniela Matei, Katharina Meraner, Uwe Mikolajewicz, Kameswarrao Modali, Wolfgang Müller, Julia Nabel, Dirk Notz, Karsten Peters-von Gehlen, Robert Pincus, Holger Pohlmann, Julia Pongratz, Sebastian Rast, Hauke Schmidt, Reiner Schnur, Uwe Schulzweida, Katharina Six, Bjorn Stevens, Aiko Voigt, and Erich Roeckner. MPI-M MPIESM1.2-HR model output prepared for CMIP6 HighResMIP, 2017. URL <https://doi.org/10.22033/ESGF/CMIP6.762>.

Wikipedia contributors. "Geography of Sudan — Wikipedia, The Free Encyclopedia", 2022. URL https://en.wikipedia.org/w/index.php?title=Geography_of_Sudan&oldid=1087952914. [Online; accessed 24-May-2022].

World Population Review. "Sudan — Wikipedia, The Free Encyclopedia", 2022. URL <https://worldpopulationreview.com/countries>. [Online; accessed 17-May-2022].

Tongwen Wu, Rucong Yu, Yixiong Lu, Weihua Jie, Yongjie Fang, Jie Zhang, Li Zhang, Xiaoge Xin, Laurent Li, Zaizhi Wang, et al. BCC-CSM2-HR: a high-resolution version of the Beijing Climate Center Climate System Model. *Geoscientific Model Development*, 14(5):2977–3006, 2021.

Sumaya Ahmed Zakieldeen. "*Adaptation to Climate Change: A Vulnerability Assessment for Sudan*". 2009.

Liu Zhenmin and Patricia Espinosa. Tackling climate change to accelerate sustainable development. *Nature Climate Change*, 9(7):494–496, 2019.

Magdi ME Zumrawi and Omer SM Hamza. Improving the characteristics of expansive subgrade soils using lime and fly ash. 2014.